

## A new fluorescent nano-chemosensor using a N<sub>2</sub>O<sub>2</sub> type macrocyclic ligand

Reza Azadbakht\* and Javad Khanabadi

Department of chemistry, Payame Noor University, Tehran, Iran

Article history:

Received: 28 April 2013

Received in revised form: 13 August 2013

Accepted: 26 August 2013

### Abstract

A new fluorescent nano-chemosensor (L) has been synthesized and characterized by <sup>1</sup>H NMR, <sup>13</sup>C NMR, COSY, HSQC, DEPT, IR spectroscopy, elemental analyses and scanning electron microscopy. The fluorescent nano-chemosensors with size about 30 nm were prepared by nanoprecipitation method. The chemosensor L showed selectivity to Al<sup>3+</sup> and Cr<sup>3+</sup> cations in EtOH/H<sub>2</sub>O (1:1, v/v) mixture. This chemosensor also exhibited an improved sensitivity and selectivity to Al<sup>3+</sup> and Cr<sup>3+</sup> cations when used as insoluble nanoparticles in aqueous buffer solution.

**Keywords:** Al<sup>3+</sup> sensor, Cr<sup>3+</sup> sensor, macrocyclic receptor, fluorescent nano-chemosensor, naphthalene

### 1. 1. Introduction

Nanotechnology is a rapidly evolving research area that utilizes nanoparticles in the development of imperative applications such as drug delivery, imaging, catalysis and chemical and biochemical sensing [1-4]. Various methods are available for the preparation of nanoparticles. Nanoprecipitation by Rapid precipitation from an organic solvent into an aqueous anti-solvent has proven an attractive processing scheme for the preparation of nanoparticles. The method is simple, rapid, economic, and requires low amounts of organic solvents. Nanoparticles have been used extensively as sensors with tremendous selectivity and sensitivity. Mostly, nanoparticles provide a signaling sub-unit for a wide range of organic and bio-chemical ligands and therefore act as excellent sensors [5]. However, most of the common nanochemosensors are made up of incorporation of a receptor on to the surface of nanoparticles. Less attention has been focused on the nanochemosensors that their receptors are nanoparticles and can act as sensor [6].

Herein, we report the synthesis of a new macrocyclic chemosensor which has two etheric oxygen atoms and two secondary amine groups as the binding sites and naphthalene moieties as the signaling units. The optical sensing ability of the chemosensor L was studied either as solution in

EtOH/H<sub>2</sub>O mixture or as insoluble nanoparticles in aqueous buffer solution. The chemosensor exhibited an improved sensitivity and selectivity to Aluminum and chromium ions when used as insoluble nanoparticles in aqueous buffer solution.

### 2. Experimental

#### 2.1. Materials and instruments

All solvents were of reagent grade quality and purchased commercially. ethane-1,2-diamine was obtained from Merck and was used without further purification. Dialdehyde D was prepared using the literature method [8]. NMR spectra were obtained using a Bruker A V500 MHz spectrometer. Infrared spectra were recorded as KBr pellets using a BIO-RAD FTS-40A spectrophotometer (4000–400 cm<sup>-1</sup>). UV–Vis absorption spectra were obtained on a Varian Cary Eclipse 300 spectrophotometer. The fluorescence spectra were recorded on a Varian spectrofluorimeter. Both excitation and emission bands were set at 5 nm. The samples were characterized by a scanning electron microscope (SEM) (Philips XL 30 and S-4160) with gold coating. Mass spectra were recorded on a JEOL JMS-SX102A.

#### 2.2. Synthesis of Dialdehyde D

1,2-Bis(bromomethyl)benzene (2.62 g, 10 mmol), 2-hydroxy-1-naphthaldehyde (3.44 g, 20 mmol) and potassium carbonate (2.79 g, 20 mmol)

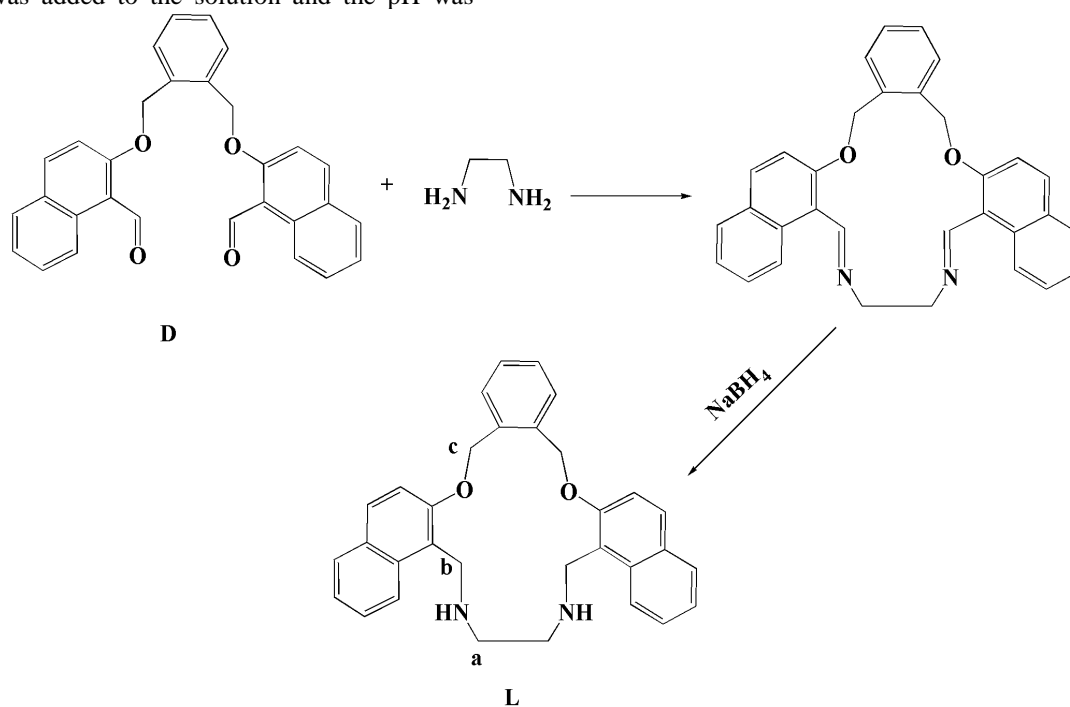
\*. Corresponding author: E-mail address: r\_azadbakht@yahoo.com Tel.: +98 812 5221144.

were dissolved in acetonitrile (300 mL). The mixture was refluxed for 48 h. The solution was then allowed to cool and the product formed as colourless crystals. (3.3 g, yield: 72%). Anal. Calcd. for  $C_{30}H_{22}O_4$ : C, 80.70; H, 4.97. Found: C, 80.84; H, 5.03. FT-IR (KBr),  $cm^{-1}$ : 1682 (C=O).  $^1H$  NMR ( $CDCl_3$ , 500 MHz)  $\delta$  (ppm): 5.34 (s, 4H, O-CH<sub>2</sub>-Ar), 7.21-9.1 (m, 12H, Ar), 10.95 (s, 2H, CH=O).

### 2.3. Synthesis of Macrocycle L

To a stirred mixture of dialdehyde D (0.447 g, 1 mmol) in methanol (100mL) was added ethane-1,2-diamine (0.063 g, 1 mmol) in methanol (10 ml). The mixture was refluxed for 2 day. The solution was then allowed to cool to room temperature after which sodium borohydride (1 g) was added in small portions to the stirred solution over 5 min. Excess water was added to the solution and the pH was

adjusted to 11 with potassium hydroxide. The solution was extracted with chloroform ( $\times 3$ ). The chloroform extracts were combined and dried over anhydrous sodium sulfate. The dried extracts were then reduced to a small volume on a rotary evaporator. The product formed as white crystals on letting this solution stand; (yield: 75%). Anal. Calcd. for  $C_{32}H_{30}N_2O_2$ : C, 80.98; H, 6.37; N, 5.90. Found: C, 80.98; H, 6.45; N, 6.00 %; FT-IR (KBr),  $cm^{-1}$ : 3250 (v NH).  $^1H$  NMR ( $CDCl_3$ , 500MHz)  $\delta$  (ppm): 1.79 (b, 2H, NH), 2.87 (s, 4H, N-CH<sub>2</sub>-CH<sub>2</sub>-N), 4.18 (s, 4H, N-CH<sub>2</sub>-Ar), 5.37 (s, 4H, O-CH<sub>2</sub>-Ar), 7.37-7.79 (m, 16H, Ar).  $^{13}C$  NMR ( $CDCl_3$ , 300MHz)  $\delta$  (ppm): 42.98, 48.45, 71.09, 116.27, 123.12, 123.83, 126.79, 128.48, 128.58, 129.19, 129.24, 129.80, 133.25, 135.53 and 154.74. The mass spectrum showed peak at  $m/z = 474$  corresponding to the [1+1] macrocycle.



Scheme 1. The synthetic route and numbering scheme for the proton assignments of L.

### 2.4. Theoretical calculations

The geometry of macrocycle L and  $[AIL]^{3+}$  were fully optimized at DFT [9,10] levels of theory using the GAUSSIAN 03 program [11], on a Pentium-PC computer with a 4000 MHz processor. A starting semi-empirical structure was optimized using the HYPERCHEM 5.02 series of programs [12].

### 2.5. Nanoparticle synthesis

A saturated solution of L was prepared by adding excess L to 10 mL of DMF in room temperature. The solution was pumped from a small orifice (a sharp needle is arranged at the front of the orifice) into 100 ml of the antisolvent (water)

which was placed in an ultrasonic bath at 180 W for 30 minutes and continuously stirred. The suspension was centrifuged at 5000 g for 15 min, and the supernatant was withdrawn and filtered through 0.2  $\mu m$  pore size syringe filter.

## 3. Results and discussion

### 3.1. Synthesis and characterization

The synthesis of macrocycle L was achieved as shown in Scheme 1. Macrocycle of L was prepared by direct cyclocondensation between the dialdehyde D and 1,2-diaminoethane in methanol, followed by reduction with NaBH<sub>4</sub> [8]. Macrocycle of L was characterized by microanalysis, mass

spectrometry, IR, and NMR studies. The macrocycle is soluble in polar solvents such as chloroform and ethanol and was hydrolytically stable under both basic and acidic conditions. The  $^1\text{H}$  and  $^{13}\text{C}$  signals were assigned using one- and two-dimensional  $^1\text{H}$ - $^1\text{H}$  COSY,  $^1\text{H}$ - $^{13}\text{C}$  HSQC and DEPT spectra. The  $^1\text{H}$  NMR spectrum of the L showed a broad signal at *ca.* 1.79 ppm attributed to secondary amine protons (2H), a singlet signal at 2.87 ppm which can be assigned to  $\text{H}_a$  (4H), a singlet signal at *ca.* 4.18 ppm attributed to  $\text{H}_b$  (4H) and a singlet signal due to the  $\text{H}_c$  (4H) resonance at *ca.* 5.37 ppm. In the aromatic region (7.37–7.79 ppm) five signals were found, and since the protons did not show scalar-coupling we were not able to assign explicitly the signals to each of the aromatic systems present in the molecule. The  $^{13}\text{C}$  NMR

spectrum in the region of aliphatic showed three signals at 42.98, 48.45 and 71.09 ppm attributed to  $\text{C}_b$ ,  $\text{C}_a$  and  $\text{C}_c$ , respectively. In the region corresponding to the signals of aromatic ring carbons (116.27–154.74 ppm), 12 peaks are observed (Figs. S 1-4).

### 3.2. Theoretical study

The resulting structure for  $[\text{AIL}]^{3+}$  was used for further calculations using the effective core potential (ECP) standard basis set LanL2DZ for Al(III) ion and the standard 6-31G\* basis set for all other atoms [13-15]. The resulting structural diagrams are shown in Fig. 1 and selected calculated bond distances and angles relating to them are shown in Table 1.

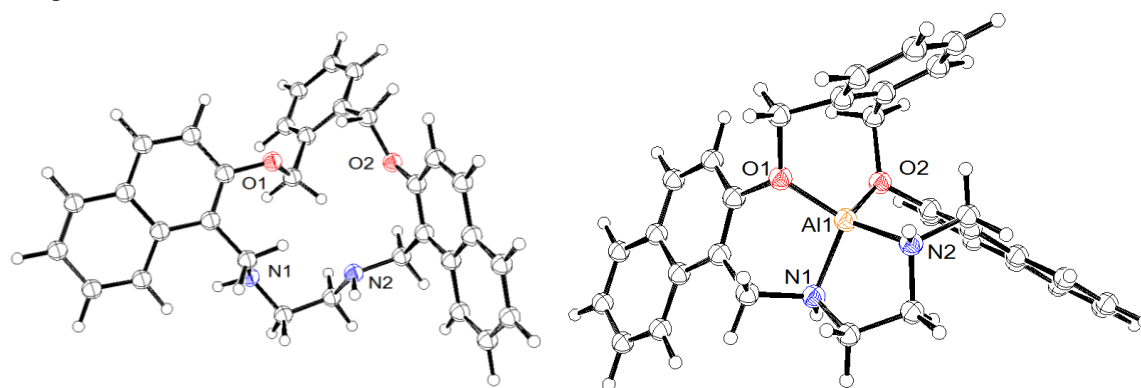


Figure 1. The DFT optimized structure of L and  $[\text{AIL}]^{3+}$ .

Table 1. Selected bond distances and angles relating for  $[\text{AIL}]^{3+}$ .

Bond Length (Å)		Bond Angle (°)	
Al(1)-O(1)	1.789	O(1)-Al(1)-O(2)	101.52
Al(1)-O(2)	1.802	O(1)-Al(1)-N(1)	101.94
Al(1)-N(1)	1.931	N(1)-Al(1)-N(2)	100.18
Al(1)-N(2)	1.93	N(2)-Al(1)-O(2)	99.94
		O(1)-Al(1)-N(2)	129.61
		O(2)-Al(1)-N(1)	136.53
<b>L</b>			
O(1)-O(2)	3.461		
O(1)-N(1)	3.588		
N(1)-N(2)	3.053		
O(2)-N(2)	3.374		
O(1)-N(2)	3.984		
O(2)-N(1)	5.312		

### 3.3. Creating supersaturation

Nanoparticles of L were prepared by Nanoprecipitation method [6]. Nanoprecipitation is an efficient technique for the preparation of versatile organic nanoparticles. The nucleation and growth kinetics dictate the final particle size and

the size distribution and are controlled via supersaturation, which can be achieved by controlling process parameters and by modifying solubility of the compound.

There are two major processing techniques for inducing supersaturation of compounds.

Traditionally, temperature quenching has been applied to create micro-scale powders with narrow size distributions while antisolvent addition has emerged as an approach to achieve much higher supersaturations for the production of nanoparticles.

Antisolvent addition technique can be achieved by the addition of an antisolvent to the solution to reduce solubility, or the reverse, diluting the dissolved compound into an antisolvent [16-19].

In this way, mild temperatures may be maintained and supersaturations high enough to yield nanoparticles are attainable. Though high supersaturation decreases both the size of the critical nucleus and increases the nucleation rate, it demands processes with very short characteristic mixing times to ensure a suitable particle size distribution.

Nanoparticles of L with mean size in the range 23-35 nm were prepared as shown in Fig. 2. The molecular states of the bulk and nanosized L were studied by means of FT-IR. Fig. 3 shows the FT-IR spectrum of the L in the range of 400–4000  $\text{cm}^{-1}$ . The spectrum of the L is characterized by the bending vibration of NH ( $1623 \text{ cm}^{-1}$ ) and stretching vibration of NH ( $3254 \text{ cm}^{-1}$ ). The close agreement between the FT-IR spectra of the raw and nanosized L suggested that there were no changes in the L molecular structure caused by the nanoprecipitation process (Fig. 3).

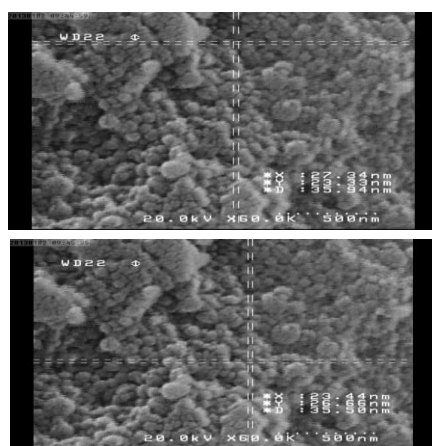


Figure 2. FTSEM images of L nanoparticles.

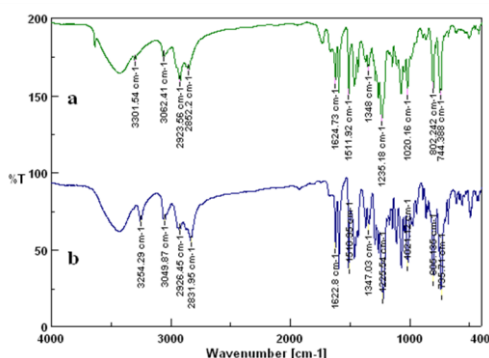


Figure 3. IR spectra of (a) nano-particles of L, (b) bulk materials of L.

### 3.4. Spectral properties of fluorescent macrocycle L

Spectral properties of fluorescent macrocycle L were studied either as solution in EtOH/ $\text{H}_2\text{O}$  mixture or insoluble nanoparticles in aqueous buffer solution. Macrocycle L shows a fluorescence emission band centered at 360 nm, with a corresponding excitation maximum at 280 nm and a Stokes shift of 80 nm.

To probe the optimum condition for the photophysical properties of the fluoroionophore prepared, the pH responses were examined either as solution in EtOH/ $\text{H}_2\text{O}$  or as insoluble nanoparticles in aqueous buffer solution (Fig. 4). In the basic condition (pH 8–12), weak fluorescent emission was observed (OFF state) due to the photo-induced electron transfer (PET) quenching by the lone pair of electrons on the secondary N donor atoms in the macrocycle. However, in the pH range of 1.0–6.0, the typical naphthalene emission was observed. Based on above results, we employed the pH 7.8 condition buffered by HEPES for the measurements of the photophysical properties throughout this study. Under this physiological condition, as expected, L exhibit negligible fluorescence emission.

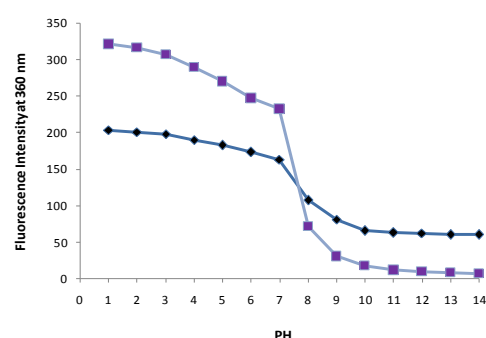


Figure 4. Fluorescence response of L in the absence of metal ions as solution in EtOH/ $\text{H}_2\text{O}$  mixture ( $\blacklozenge$ ) and as insoluble nanoparticles in aqueous solution ( $\blacksquare$ ) at different pH values

The optical sensing ability of L was studied by addition of metal ions such as  $\text{Na}^+$ ,  $\text{K}^+$ ,  $\text{Cs}^+$ ,  $\text{Mg}^{2+}$ ,  $\text{Ba}^{2+}$ ,  $\text{Al}^{3+}$ ,  $\text{Pb}^{2+}$ ,  $\text{Cr}^{3+}$ ,  $\text{Mn}^{2+}$ ,  $\text{Fe}^{3+}$ ,  $\text{Fe}^{2+}$ ,  $\text{Co}^{2+}$ ,  $\text{Ni}^{2+}$ ,  $\text{Cu}^{2+}$ ,  $\text{Zn}^{2+}$ ,  $\text{Cd}^{2+}$ ,  $\text{Hg}^{2+}$  and  $\text{Ag}^+$  in EtOH/ $\text{H}_2\text{O}$  mixture (PH = 7.8). Emission responses of L as solution in EtOH/ $\text{H}_2\text{O}$  mixture is shown in Figure 5a. Significantly, when increasing concentrations of  $\text{Al}^{3+}$  or  $\text{Cr}^{3+}$  ions were introduced, the emission of L was increased. No significant changes in fluorescence were observed in the experiments with  $\text{Na}^+$ ,  $\text{K}^+$ ,  $\text{Ba}^{2+}$ ,  $\text{Mg}^{2+}$  and  $\text{Mn}^{2+}$ . Treatment with  $\text{Zn}^{2+}$  and  $\text{Cd}^{2+}$  generated some fluorescence centered at 360 nm, but the intensity was lower than with  $\text{Al}^{3+}$  and  $\text{Cr}^{3+}$  under the same conditions. The weak fluorescence of L was completely quenched by addition of  $\text{Fe}^{2+}$  and  $\text{Fe}^{3+}$  ions. The fluorescence intensity of L was decreased in the presence of the other ions.

Emission responses of insoluble nanoparticles L in the presence of different metal ions in aqueous buffer solution (PH = 7.8) are shown in Fig. 5b. As it can be seen from Figure 4b, when increasing concentrations of  $\text{Al}^{3+}$  or  $\text{Cr}^{3+}$  ions were introduced, the emission of L was drastically increased. The weak fluorescence of nanoparticles L was completely quenched by addition of  $\text{Fe}^{2+}$ ,  $\text{Fe}^{3+}$  and  $\text{Cu}^{2+}$  ions. No significant changes were observed in the experiments of nanoparticles L in the presence of the other ions.

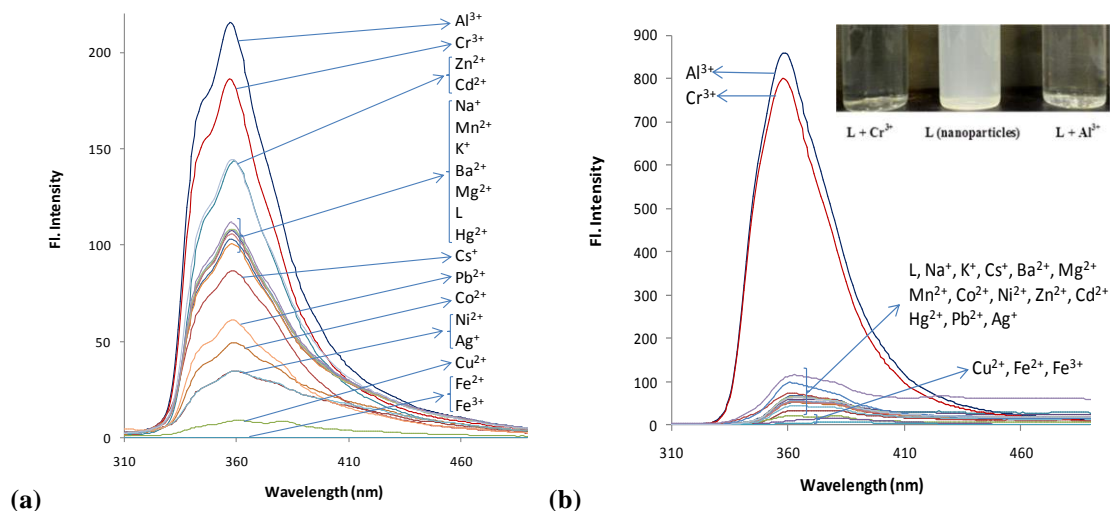


Figure 5. Fluorescence spectra of L (a) in the presence of various metal ions  $\text{Na}^+$ ,  $\text{K}^+$ ,  $\text{Cs}^+$ ,  $\text{Mg}^{2+}$ ,  $\text{Ba}^{2+}$ ,  $\text{Al}^{3+}$ ,  $\text{Pb}^{2+}$ ,  $\text{Cr}^{3+}$ ,  $\text{Mn}^{2+}$ ,  $\text{Fe}^{3+}$ ,  $\text{Fe}^{2+}$ ,  $\text{Co}^{2+}$ ,  $\text{Ni}^{2+}$ ,  $\text{Cu}^{2+}$ ,  $\text{Zn}^{2+}$ ,  $\text{Cd}^{2+}$ ,  $\text{Hg}^{2+}$  and  $\text{Ag}^+$  ( $100\mu\text{M}$ ) in EtOH/ $\text{H}_2\text{O}$  mixture, (b) as nanoparticles in aqueous buffer solution.

It is shown here that the free ligand L exhibits low fluorescence due to photoinduced electron transfer (PET) but specifically in presence of  $\text{Al}^{3+}$  and  $\text{Cr}^{3+}$  ions, the remarkable fluorescence enhancement of macrocycle L was mainly induced by residing of aluminum ions within the macrocyclic cavity of L and binding with the donor nitrogen atoms. Upon complexation with  $\text{Al}^{3+}$  or  $\text{Cr}^{3+}$  ions the intramolecular PET fluorescence quenching effect could be relieved by reducing the electron density of lone pairs through metal–donor binding interaction and thus increases the ligand emission.

When the metal ions were added to insoluble nanoparticles in aqueous buffer solution, only in the presence of  $\text{Fe}^{2+}$ ,  $\text{Fe}^{3+}$ ,  $\text{Al}^{3+}$  and  $\text{Cr}^{3+}$  ions the insoluble nanoparticles were solved.

$\text{Fe}^{2+}$  and  $\text{Fe}^{3+}$  ions quench the fluorescence of chemosensor either as solution in EtOH/ $\text{H}_2\text{O}$  or as insoluble nanoparticles in aqueous buffer solution. As shown in Figs 4 and 5, the chemosensor when used as nonparticles is more sensitive than when used as solution (for  $\text{Al}^{3+}$  and  $\text{Cr}^{3+}$  ions).

The FEF (fluorescence enhancement factor) values of fluorescent macrocycles L responding to different metal ions either as solution in EtOH/ $\text{H}_2\text{O}$  or insoluble nanoparticles in aqueous buffer solution are shown in Fig. 6a and Fig. 6b, respectively. The FEF ( $I_x - I_L$ )/ $I_L$  was calculated using minimal ( $I_L$ ) and maximal ( $I_x$ ) fluorescence intensities recorded before and after addition of metal ions, respectively. The highest fluorescence enhancement for L has been observed in the presence of  $\text{Al}^{3+}$  ions (Fig. 6).

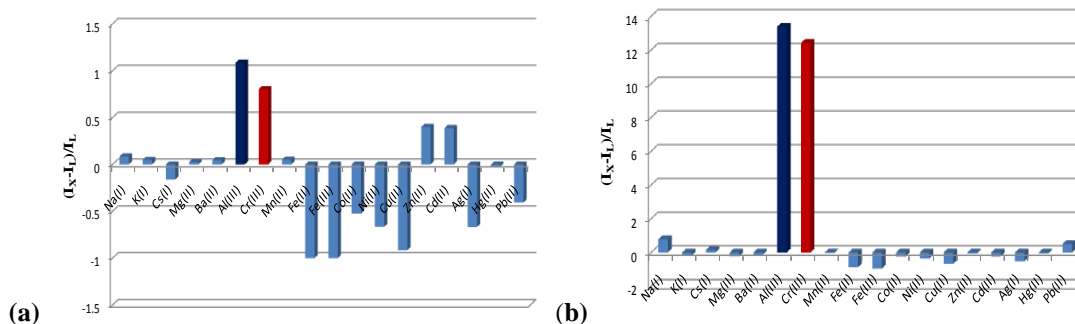


Figure 6. (a) Fold of enhancement and % quenching for different cations upon binding with macrocycle L in EtOH/ $\text{H}_2\text{O}$  mixture and (b) FEF values of nanoparticles L in buffer aqueous solution at  $25\text{ }^\circ\text{C}$ . Both the excitation and emission slit widths were 5.0 nm

To further investigate the chemosensor properties of L, we performed fluorescence titrations of insoluble nanoparticles in aqueous buffer solution in the presence of different concentrations of  $\text{Al}^{3+}$  and  $\text{Cr}^{3+}$  ions. Figure 7 shows the gradual enhancements in fluorescence intensity for L upon the addition of increasing concentrations of  $\text{Al}^{3+}$  and  $\text{Cr}^{3+}$  ions.

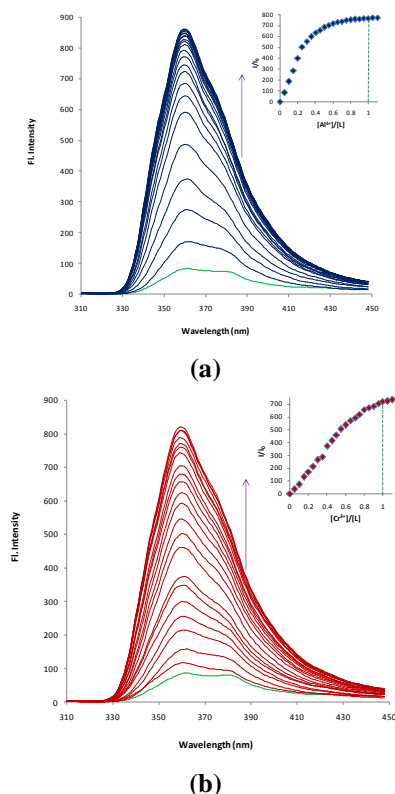


Figure 7. Changes in the fluorescence spectrum of macrocycle L ( $10\mu\text{M}$ ) as a function of added  $\text{Al}^{3+}$  concentration ( $0\text{--}12\mu\text{M}$ ) in ethanol (a) and as insoluble nanoparticles in aqueous buffer solution (b). Excitation wavelength was  $280\text{ nm}$ . Both the excitation and emission slit widths were  $5.0\text{ nm}$ .

In order to determine the stoichiometry of the  $\text{L-Al}^{3+}$  and  $\text{L-Cr}^{3+}$  complexes, the Job's method was used [20,21]. In the Job's plot (Fig. 8), a maximum fluorescence change was observed with a  $0.5\text{ M}$  fraction of ionophore to  $\text{Al}^{3+}$  for L, which indicated that only a  $1:1$  complex was formed. A similar result was found to chromium ions.

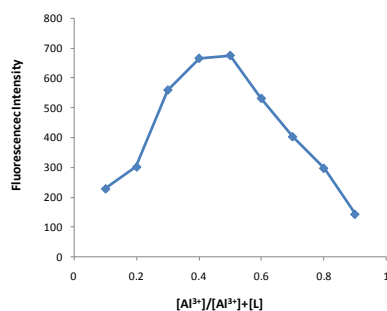


Figure 8. Job's plot for  $\text{L} + \text{Al}^{3+}$ .

The absorption spectrum of L exhibited structured absorption spectrum corresponding to the  $\pi\text{-}\pi^*$  transitions of naphthalene unit observed in naphthalene derivatives. However, the change in the environment of the naphthalene unit in the present systems L caused changes in the intensities and positions of the  $\pi\text{-}\pi^*$  bands compared to that of pure naphthalene.

The absorption spectra of L are based on the naphthalene moiety and are slightly dependent on the addition of  $\text{Al}^{3+}$  or  $\text{Cr}^{3+}$  ions to the macrocyclic skeleton. Changes of the absorption spectra of macrocycles L upon addition of  $\text{Al}^{3+}$  ions are shown in Fig. 9.

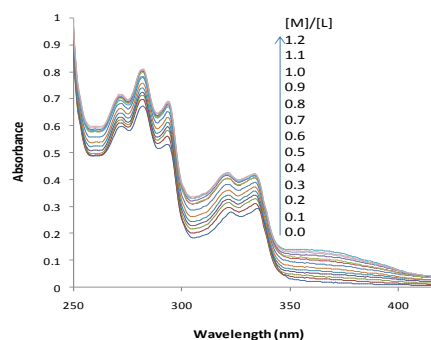


Figure 9. Changes absorption spectrum of macrocycle L ( $10\mu\text{M}$ ) as a function of added  $\text{Al}^{3+}$  concentration in ethanol.

#### 4. Conclusion

In Conclusion, The cyclocondensation of dialdehyde D with ethane-1,2-diamine, followed by an in situ reduction with  $\text{NaBH}_4$  yielded the new fluorescence macrocyclic chemosensor (L) containing two naphthalene fluorophores. The fluorescent nano-chemosensors with size about  $30\text{ nm}$  were prepared by nanoprecipitation method. Nanoparticles L possesses a high affinity and selectivity for aluminum and chromium ions relative to most other competitive metal ions like  $\text{Na}^+$ ,  $\text{K}^+$ ,  $\text{Cs}^+$ ,  $\text{Mg}^{2+}$ ,  $\text{Ba}^{2+}$ ,  $\text{Pb}^{2+}$ ,  $\text{Mn}^{2+}$ ,  $\text{Fe}^{3+}$ ,  $\text{Fe}^{2+}$ ,  $\text{Co}^{2+}$ ,  $\text{Ni}^{2+}$ ,  $\text{Cu}^{2+}$ ,  $\text{Zn}^{2+}$ ,  $\text{Cd}^{2+}$ ,  $\text{Hg}^{2+}$  and  $\text{Ag}^+$  by enhancement of the fluorescence emission at  $360\text{ nm}$ .

#### 5. Acknowledgment

We are grateful to the Department of Chemistry of Payame Noor University and Ministry of Science Research and Technology for the financial support.

#### References

- [1] (A) S. Aryal, C. M. J. Hu and L. Zhang, *Mol. Pharm.* **8** (2011) 1401. (b) S. D. Brown, P. Nativo, J.-A. Smith, D. Stirling, P. R. Edwards, B. Venugopal, D. J. Flint, J. A. Plumb, D. Graham and N. J. Wheate, *J. Am. Chem. Soc.* **132** (2010) 4678. (c) S. Kim, K. Seong, O. Kim, S. Kim, H. Seo, M. Lee, G. Khang and D. Lee, *Biomacromolecules*. **11** (2010) 555.

- [2] (a) X. Gao, J. Chen, B. Wu, H. Chen and X. Jiang, *Bioconjugate Chem.* **19** (2008) 2189. (b) C. M. Lee, D. R. Jang, J. Kim, S. J. Cheong, E. M. Kim, M. H. Jeong, S. H. Kim, D.W. Kim, S.T. Lim, M. H. Sohn, Y.Y. Jeong and H. J. Jeong, *Bioconjugate Chem.* **22** (2011) 186.
- [3] (a) M. H. Oh, N. Lee, H. Kim, S.P. Park, Y. Piao, J. Lee, S. W. Jun, W. K. Moon, S. H. Choi and T. Hyeon, *J. Am. Chem. Soc.* **133** (2011) 5508. (b) M. Moreno-Manas and R. Pleixats, *Acc. Chem. Res.* **36** (2003) 638. (c) R. Narayanan, M. A. El-Sayed, *J. Phys. Chem. B* **109** (2005) 12663. (d) M. C. Daniel, D. Astruc, *Chem. Rev.* **104** (2004) 293. (e) C. Burda, X. Chen, R. Narayanan and M. A. El-Sayed, *Chem. Rev.* **105** (2005) 1025.
- [4] (a) S. Lal, S. Link and N. J. Halas, *Nat. Photonics.* **1** (2007) 641. (b) S.V. Kyriacou, W. J. Brownlow and X. H. N. Xu, *Biochemistry.* **43** (2004) 140. (c) K. Aslan, J. R. Lakowicz and C. D. Geddes, *Anal. Chem.* **77** (2005) 2007.
- [5] (a) H. B. Na, G. Palui, J. T. Rosenberg, S. C. Grant and H. Mattoussi, *ACS Nano.* **6** (2012) 389. (b) R. K. O'Reilly, C. J. Hawker and K. L. Wooley, *Chem. Soc. Rev.* **35** (2006) 1068. (c) M. Halimani, S. P. Chandran, S. Kashyap, V. M. Jadhav, B. L. V. Prasad, S. Hotha and S. Maiti, *Langmuir.* **25** (2009) 2339. (d) H. D. Na, G. Pauli, J. T. Rosenberg, X. Ji, S. C. Grant and H. Mattoussi, *ACS Nano.* **6** (2012) 389.
- [6] R. Azadbakht and J. Khanabadi, *Tetrahedron.* **69** (2013) 3206.
- [7] (a) M. Dong, Y. M. Dong, T. H. Ma, Y. W. Wang and Y. Peng, *Inorg. Chim. Acta.* **381** (2012) 137. (b) C. Gou, S. H. Qin, H. Q. Wu, Y. Wang, J. Luo and X. Y. Liu, *Inorg. Chem. Commun.* **14** (2011) 1622. (c) K. Kaur, V. K. Bhardwaj, N. Kaur and N. Singh, *Inorg. Chem. Commun.* **26** (2012) 31. (d) S. H. Kim, H. S. Choi, J. Kim, S. J. Lee, D.T. Quang and J. S. Kim, *Org. Lett.* **12** (2010) 560. (e) D. Maity and T. Govindaraju, *Chem. Commun.* **46** (2010) 4499. (f) A. B. Othman, J. W. Lee, Y. D. Huh, R. Abidi and J. S. Kim, J. Vicens, *Tetrahedron.* **63** (2007) 10793. (g) Y. Zhao, Z. Lin, H. Liao, C. Duan and Q. Meng, *Inorg. Chem. Commun.* **9** (2006) 966.
- [8] R. Azadbakht and J. Khanabadi, *Inorg. Chem. Commun.* **30** (2013) 21.
- [9] A. D. Becke, *J. Chem. Phys.* **98** (1993) 5648.
- [10] C. Lee, W. Yang and R. G. Parr, *Phys. Rev. B.* **37** (1988) 785.
- [11] M. J. Frisch, G. W. Trucks, H. B. Schlegel, G. E. Scuseria, M. A. Robb, J. R. Cheeseman, J. A. Montgomery, Jr., T. Vreven, K. N. Kudin, J. C. Burant, J. M. Millam, S. S. Iyengar, J. Tomasi, V. Barone, B. Mennucci, M. Cossi, G. Scalmani, N. Rega, G. A. Petersson, H. Nakatsuji, M. Hada, M. Ehara, K. Toyota, R. Fukuda, J. Hasegawa, M. Ishida, T. Nakajima, Y. Honda, O. Kitao, H. Nakai, M. Klene, X. Li, J. E. Knox, H. P. Hratchian, J. B. Cross, V. Bakken, C. Adamo, J. Jaramillo, R. Gomperts, R. E. Stratmann, O. Yazyev, A. J. Austin, R. Cammi, C. Pomelli, J. W. Ochterski, P. Y. Ayala, K. Morokuma, G. A. Voth, P. Salvador, J. J. Dannenberg, V. G. Zakrzewski, S. Dapprich, A. D. Daniels, M. C. Strain, O. Farkas, D. K. Malick, A. D. Rabuck, K. Raghavachari, J. B. Foresman, J. V. Ortiz, Q. Cui, A. G. Baboul, S. Clifford, J. Cioslowski, B. B. Stefanov, G. Liu, A. Liashenko, P. Piskorz, I. Komaromi, R. L. Martin, D. J. Fox, T. Keith, M. A. Al-Laham, C. Y. Peng, A. Nanayakkara, M. Challacombe, P. M. W. Gill, B. Johnson, W. Chen, M. W. Wong, C. Gonzalez, and J. A. Pople, *Gaussian, Inc., Pittsburgh PA*, 2003.
- [12] Hyperchem, Release 5.02; Hypercube: Gainesville, FL, (1997).
- [13] K. D. Dobbs and W. J. Hehre, *J. Comp. Chem.* **8** (1987) 880.
- [14] P. J. Hay and W. R. Wadt, *J. Chem. Phys.* **82** (1985) 299.
- [15] P. C. Hariharan and J. A. Pople, *Theor. Chim. Acta.* **28** (1973) 213.
- [16] B. K. Johnson and R. K. Prud'homme, *Aust. J. Chem.* **56** (2003) 1021.
- [17] M. E. Matteucci, M. A. Hotze, K. P. Johnston and R. O. Williams, *Langmuir.* **22** (2006) 8951.
- [18] H. Zhao, J. X. Wang, Q. A. Wang, J. F. Chen and J. Yun, *Ind. Eng. Chem. Res.* **46** (2007) 8229.
- [19] M. Kakran, N. G. Sahoo, L. Li, Z. Judeh, Y. Wang, K. Chong and L. Loh, *Int. J. Pharm.* **383** (2010) 285.
- [20] W. C. Vosburgh and G. R. Cooper, *J. Am. Chem. Soc.* **63** (1941) 437.
- [21] R. R. Avirah, K. Jyothish and D. Ramaiah, *Org. Lett.* **9** (2007) 121.

